

## Preliminary evaluation of image reconstruction by ordered-subset expectation maximization in thallium-201 lung scintigraphy

Jingming BAI, Kunihiro YOKOYAMA, Seigo KINUYA, Kenichi NAKAJIMA, Masato YAMADA,  
Kenji ICHIYANAGI, Takatoshi MICHIGISHI and Norihisa TONAMI

*Department of Biotracer Medicine, Graduate School of Medical Sciences, Kanazawa University*

**Objectives:** We observed whether clearer tumor delineation and greater tumor to non-tumor (T/N) count ratios could be obtained using an iterative ordered-subsets expectation maximization (OSEM) algorithm than conventional filtered-back projection algorithm (FBP) in the image reconstruction of thallium-201 ( $^{201}\text{Tl}$ ) lung scintigraphy. **Methods:** In 29 patients with lung cancer and phantom studies, tomograms were reconstructed using FBP and OSEM algorithms, with and without a prefilter (Butterworth filter: BW), whose cut-off frequencies were 0.10 cycles/pixel for FBP and 0.10 and 0.17 cycles/pixel for OSEM. Visual interpretation and tumor to non-tumor (T/N) count ratios were obtained and compared. **Results:** Without a prefilter, T/N ratios from OSEM and FBP were  $1.89 \pm 0.31$  (early) and  $2.00 \pm 0.54$  (late) for OSEM,  $1.90 \pm 0.33$  (early) and  $2.05 \pm 0.59$  (late) for FBP, respectively. The OSEM reconstruction without prefiltering showed clearer tumor contours than FBP without a prefilter. Incorporation of BW showed visually low-noised images but decreased T/N ratios in both reconstructions with BW (0.10 cycles/pixel). No greater T/N ratios were obtained by OSEM than FBP, with or without prefiltering. With BW with a cut-off frequency of 0.17 cycles/pixel, the same T/N ratios as those without BW were obtained. The tumor model sized 0.9 cm in the phantom study was invisible in both OSEM and FBP reconstructions without a prefilter, but visible with a prefilter. The influence of prefiltering on T/N ratios was also observed in phantom studies. **Conclusions:** Visually improved tumor delineation could be obtained in OSEM reconstruction without a prefilter as compared to FBP reconstruction without a prefilter for tumors greater than 2 cm. Prefiltering should be incorporated into OSEM reconstruction in diagnosing small tumors. However, the influence of prefilter (BW) setting on semi-quantitative interpretation needs further discussion.

**Key words:**  $^{201}\text{Tl}$  scintigraphy, lung cancer, image reconstruction, OSEM algorithm

### INTRODUCTION

LUNG CANCER is increasing in incidence throughout the world and is one of the major causes of death in many countries.<sup>1</sup> Up to now, thallium-201 ( $^{201}\text{Tl}$ ), Tc-99m labeled tracers such as sestamibi, tetrofosmin and  $^{18}\text{F}$ -FDG have been used for lung nodule characterization or pretherapeutic staging. Thallium-201 accumulates in

viable tumor tissues, depending on the proliferative potential of tumor cells.<sup>2–4</sup> Malignant lung tumors usually have relatively high and prolonged uptake, while benign lesions have relatively low uptake and fast clearance.<sup>5,6</sup> Now, despite its many inferior properties,  $^{201}\text{Tl}$  scintigraphy is still widely used,<sup>7–9</sup> since its value was first reported in the management of primary lung cancers.<sup>10</sup>

Tumor detection with  $^{201}\text{TlCl}$  depends on the uptake contrast between tumor and surrounding normal tissue, which is determined mainly by the inherent characteristics of the tumor. It is also influenced by image quality.<sup>11</sup> Lower image noise and higher T/N are usually helpful with visual interpretation of SPECT images.

The image reconstruction algorithm is a key factor for

Received June 18, 2003, revision accepted August 6, 2003.

For reprint contact: Jingming BAI, M.D., Department of Biotracer Medicine (Nuclear Medicine), Kanazawa University, 13–1 Takara-machi, Kanazawa 920–0815, JAPAN.

E-mail: bjingming@nmd.m.kanazawa-u.ac.jp

correct image interpretation. Conventionally, filtered back-projection (FBP) has been the most widely applied technique in SPECT reconstruction since the first report describing in 1974.<sup>12</sup> This FBP algorithm is linear, fast and easy to implement; however, it is prone to make image artifacts such as “line” (reconstruction process) and “cold areas” surrounding high uptake spots.<sup>13</sup> Such artifacts often cause difficulties in localizing small or low-uptake tumors.

Recently, maximum likelihood expectation maximization has become a clinically practical alternative to FBP. Its revised version, the ordered-subset expectation maximization algorithm (OSEM), is commercially available software for the triple-headed rotating gamma camera (GCA-9300A/HG, Toshiba Corporation, Tokyo, Japan). Its usefulness has been reported in many studies.<sup>14–16</sup> However, few articles concerning OSEM in <sup>201</sup>Tl lung scintigraphy have appeared in the literature.

Image noise is a troublesome problem in nuclear medicine procedures. To achieve image noise reduction in FBP reconstruction, BW prefilter has been routinely used. In OSEM reconstruction of SPECT study, although few papers discussing prefilter or postfilter are available, according to our preliminary studies in clinical practice (data not published), such a prefilter or postfilter is necessary to obtain low-noised images. Such low-noised images tend to aid in the effective identification of suspicious lesions by nuclear medicine physicians.

To observe whether clearer tumor delineation and higher tumor to non-tumor ratios can be obtained in OSEM images than in FBP images, we reconstructed images of lung cancer using OSEM and compared them with FBP in clinical and phantom studies, with and without BW.

## MATERIALS AND METHODS

### *Subjects*

#### *Clinical study*

Twenty-nine lung cancer patients undergoing <sup>201</sup>Tl lung scanning (20 men, 9 women; age range 40–82 years) with a solitary nodule in the lung field were selected for this study. Sixteen cases of adenocarcinoma, 9 of squamous carcinoma, 1 of large cell carcinoma, 2 of small cell carcinoma and 1 of adeno-squamous carcinoma were diagnosed pathologically. The tumors were greater than 2 cm in maximum diameter on post-operative specimens in all 29 cases.

#### *Phantom study*

To compare OSEM and FBP in lung tumors smaller than 2 cm in diameter, a cylindrical torso phantom measuring 20 cm in diameter and 18 cm in length (Toshiba Corporation, Tokyo, Japan) was used. Thallium-201 solution (18.5 MBq) was added to 5,500 ml of water (volume of phantom), and was homogenized to simulate lung back-

ground radioactivity. A plastic container of 5 cm in diameter, filled with 5-fold higher radioactivity than the background, was prepared as a “hot spot,” and syringes with diameters 0.1 cm, 0.9 cm, 1.2 cm, 1.4 cm, 2.0 cm and 2.9 cm filled with 4-fold higher radioactivity than background were applied as tumor models. The tumor models and hot spot were placed on the same horizontal plane and kept over 1.5 cm apart from each other.

### *Data acquisition and image reconstruction*

A triple-headed rotating gamma camera (GCA-9300A/HG, Toshiba Corporation, Tokyo, Japan) equipped with a low-energy general purpose parallel hole collimator, and a medical image processor (GMS-5500A/DI, Toshiba Corporation, Tokyo) were used for the study. The rotation radius of the three detectors ranged from 20 cm to 23 cm according to patient weight. The SPECT resolution at this rotation radius range approximated 1.5 cm. The rotation radius in the phantom study was set at 22 cm to match the SPECT resolution in the clinical study. All projection images were obtained in a matrix of 128 × 128 through the use of step-and-shoot acquisition. The size of the pixel was 3.2 mm. Since appropriate methods for attenuation correction incorporated in OSEM reconstruction were not available, we did not perform attenuation correction in the present study.

The SPECT images of patients were obtained at 15 min (early phase) and 3 hrs (late phase) after intravenous injection of 111 MBq of <sup>201</sup>Tl. The detector was rotated around the chest by 6 degrees per step with acquisition time of 50 sec for 360 degrees. The energy window was set at 71 keV with a 25% width. Scatter correction was not performed.

The images were reconstructed using both OSEM and FBP algorithms. In FBP reconstruction, after processing with a Butterworth filter (BW) of order 8 (fixed parameter) and a cut-off frequency of 0.10 cycles/pixel, which is most suitable and has been routinely applied at our institution, data were reconstructed with a ramp filter. In OSEM, to observe whether a prefilter such as BW will influence the T/N calculation, we plotted the mean T/N ratios of 3 lung cancer cases against cut-off frequencies ranging from minimum 0.07 to maximum 0.40 cycles/pixel.

Reconstructions using OSEM and FBP with and without BW (0.10 cycles/pixel) were performed in all 29 cases. OSEM reconstruction with BW (0.17 cycles/pixel) was also performed.

In most phantom and clinical studies of OSEM reconstruction, iterations ranging from 3 to 5 supplied with more than 8 views per subset have been used, despite the fact that no conclusive agreement has been reached in the setting.<sup>15,17–19</sup> We performed OSEM reconstruction using iteration 3 and subset 10.<sup>14</sup>

A focus of increased <sup>201</sup>Tl uptake was correlated with the location of the carcinoma on chest X-ray and CT.

Then, one transverse slice showing maximal activity of the tumor was selected, and a region of interest (ROI) was drawn along the margin of the lesion. A corresponding ROI was drawn in the contra-lateral normal lung field as a background ROI.

In the phantom study, image reconstruction, selection of transverse image and tumor ROI drawing were done as mentioned above, but a background ROI was drawn in the center of the transverse image because the tumor models were arranged like a circle.

The identical slice was used in the comparison between OSEM and FBP algorithms in both the clinical and phantom studies.

### Statistical methods

Statistical analysis was performed with commercially available software Statview Version 5.0 on a Macintosh personal computer. Comparison of early and late T/N ratios from FBP and OSEM were examined by Wilcoxon

paired test. P values less than 0.05 were considered significant.

## RESULTS

### Clinical study

Mean T/N ratios of three lung cancers greater than 2.0 cm in maximal diameter in the OSEM algorithm were plotted with serial BW settings of different cut-off frequencies (Fig. 1). The T/N ratios increased gradually following the alteration of the cut-off frequency from 0.07 until 0.17 cycles/pixel, and reached an approximate plateau when the cut-off frequency was equal to or greater than about 0.17 cycles/pixel.

The T/N ratios in 29 cases were summarized in Table 1. With or without BW (0.10 cycles/pixel), OSEM reconstruction did not achieve greater T/N ratios than FBP. Prefilter incorporation into FBP decreased the T/N ratios. The T/N ratios from OSEM without BW and with BW (0.17 cycles/pixel) were significantly greater than OSEM with 0.10 cycles/pixel BW ( $p < 0.05$ , respectively). The T/N ratios from OSEM with 0.17 cycles/pixel BW were not different from those from OSEM without BW.

Visually clearer tumor delineation was achieved in the OSEM images without BW than FBP without BW. No difference was visualized between OSEM and FBP when BW was incorporated into the two reconstructions. Transverse images were reconstructed using FBP and OSEM in a 59-year-old male with a solitary 2 cm adenocarcinoma in the left upper lung (Fig. 2). Without BW, OSEM images (Figs. 2 C and H) showed clear tumor contours, while FBP images did not (Figs. 2 A and F). With BW, both FBP (Figs. 2 B and G) and OSEM (Figs. 2 D, E, I and J) delineated the tumor clearly.

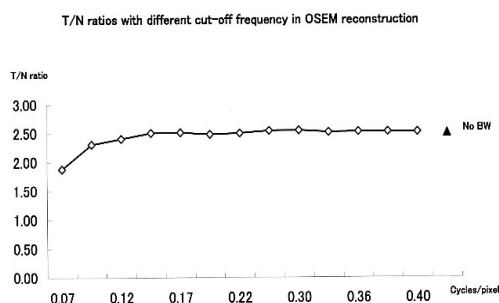


**Fig. 1** T/N ratios in OSEM images with serial cut-off frequency from 0.07 to 0.40 cycles/pixel.

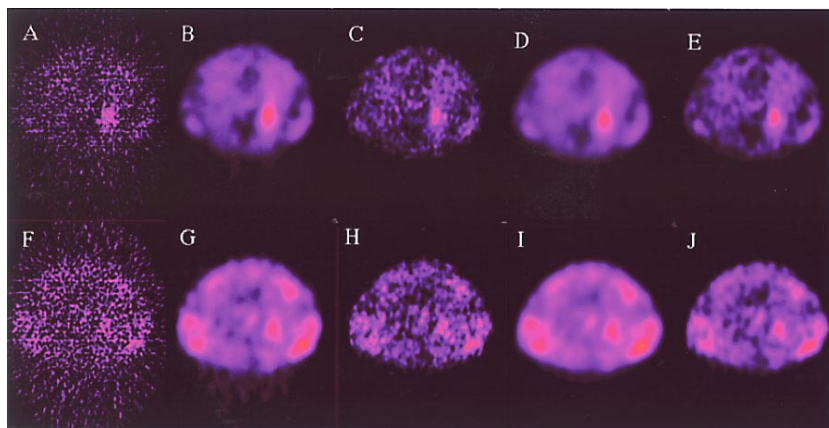


**Fig. 2** A 59-year-old man with 2 cm adenocarcinoma in the left upper lung. The early (*upper row*) and late (*lower row*) images were reconstructed using FBP and OSEM, with and without BW. A: early FBP image without BW. B: early FBP image with BW. C: early OSEM image without BW. D: early OSEM image with BW setting of cut-off frequency 0.10 cycles/pixel. E: early OSEM image with BW setting of cut-off frequency 0.17 cycles/pixel. F: late FBP image without BW. G: late FBP image with BW. H: late OSEM image without BW. I: late OSEM image with BW setting of cut-off frequency 0.10 cycles/pixel. J: late OSEM image with BW setting of cut-off frequency 0.17 cycles/pixel.

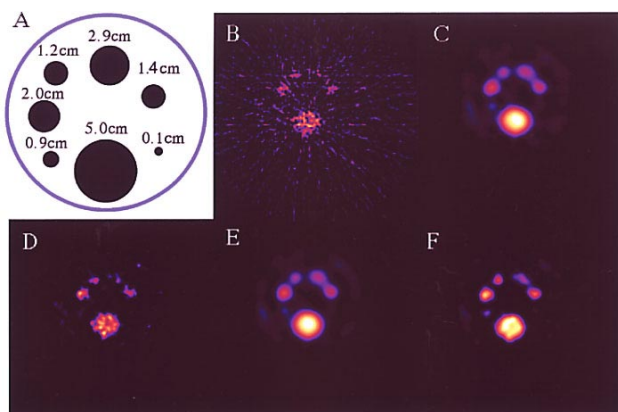


**Fig. 3** Phantom images from FBP and OSEM reconstruction, with and without BW. A: phantom scheme: the numbers show the diameter of tumor models and the hot spot. B: FBP image without BW. C: FBP image with BW (0.10 cycles/pixel). D: OSEM image without BW. E: OSEM image with BW (0.10 cycles/pixel). F: OSEM image with BW (0.17 cycles/pixel).

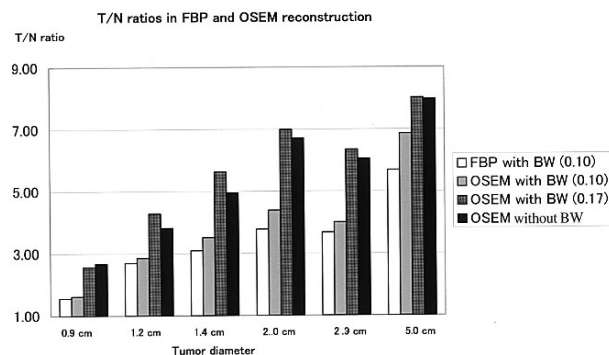


**Fig. 4** T/N ratios of tumor models in FBP and OSEM reconstruction, with and without BW (0.10 and 0.17 cycles/pixel). ( ): The number indicates the cut-off frequency (cycles/pixel) of BW. The true value of the T/N ratios is 4.0.

**Table 1** T/N ratios in 29 cases of lung cancer

BW	FBP (-)	FBP (0.10)	OSEM (-)	OSEM (0.10)	OSEM (0.17)
ER	1.90 ± 0.33	1.77 ± 0.30*	1.89 ± 0.31	1.71 ± 0.27**	1.86 ± 0.30
LR	2.05 ± 0.59	1.92 ± 0.52*	2.00 ± 0.54	1.81 ± 0.53**	1.99 ± 0.53

Legends: ( ): The number indicates the cut-off frequency (cycles/pixel) of BW; (-): Reconstruction without BW; ER: T/N ratio in early phase; LR: T/N ratio in late phase; \*: Significantly lower than FBP with BW setting of cut-off frequency 0.10 cycles/pixel; \*\*: Significantly lower than both OSEM with and without BW setting of cut-off frequency 0.17 cycles/pixel

#### Phantom study

In the visual interpretation of image quality, without BW, OSEM reconstruction produced lower-noised images than FBP. Using BW, both reconstruction images produced similar low-noised images (Fig. 3). The tumor model sized 0.9 cm was observed clearly in both OSEM and FBP with BW, but not without BW. The tumor model sized 0.1 cm was not observed even with BW.

The T/N ratios of tumors sized from 0.9 cm to 2.9 cm were obtained. The contour of tumor sized 0.9 cm in both OSEM and FBP without BW was drawn along with the one with BW because it was invisible in both OSEM and FBP without BW. All the T/N ratios of tumor models in OSEM with and without BW (0.17 cycles/pixel), were greater than OSEM with 0.10 cycles/pixel BW (Fig. 4).

Compared with the true T/N ratio (4.0), we found that different BW settings led to different calculated T/N ratios. The T/N ratios of tumor models sized 0.9 cm and 1.2 cm were much lower than 4, in both FBP and OSEM reconstruction with the cut-off frequency of 0.10 cycles/pixel. The values were improved greatly to near 4, with 0.17 cycles/pixel or without BW. The T/N ratios of tumor models sized 1.4 cm, 2.0 cm and 2.9 cm were underesti-

mated with 0.10 cycles/pixel BW. However, these values were overestimated in both OSEM with and without BW (0.17 cycles/pixel).

The T/N ratios of the “hot spot” in both FBP and OSEM reconstruction, with and without BW were all greater than the true T/N ratio (5.0).

With BW (0.10 cycles/pixel), the T/N ratios of tumor models and the “hot spot” from OSEM were slightly greater than from FBP. The T/N ratios from OSEM with BW (0.17 cycles/pixel) were also slightly higher than OSEM without BW in tumors except for the one sized 0.9 cm.

## DISCUSSION

The plot of Figure 1 demonstrated the influence of prefilter setting on T/N ratio calculation in OSEM reconstruction. This influence might also exist in FBP reconstruction. Slight alterations of T/N may not hamper the localization of lung tumors with high uptake, but the T/N change may be crucial for those with low uptake or tumor post-chemotherapeutic evaluation. Therefore, prefilter setting in OSEM should be determined properly.

Identification on nuclear medicine images is an important prerequisite for correct evaluation of suspicious lesions. It is well-known that FBP images without a prefilter can not meet the requirements of clinical practice (Fig. 2). For OSEM reconstruction, prefilter BW was unnecessary for the identification of the tumors equal to or greater than 2 cm in diameter.

However, the phantom study showed that a prefilter might be necessary in OSEM reconstruction for small tumors. The fact that the tumor model sized 0.9 cm in the phantom study was delineated clearly with BW but not without BW supported this contention.

When considering prefilter incorporation in OSEM reconstruction, the negative influence of the prefilter on T/N ratios should be eliminated because relatively high T/N ratios are essential for successful visual interpretation under some circumstances. The T/N curve (Fig. 1) and T/N ratios (Table 1) showed that an "appropriate" BW setting could avoid this influence.

In fact, appropriate prefilter determination seemed to be difficult in this study. BW (0.10 cycles/pixel) underestimated the T/N ratios of tumor sized 0.9 cm and 1.2 cm but estimated correctly the tumors 1.4 cm, 2.0 cm and 2.9 cm. BW (0.17 cycles/pixel) and absence of BW produced approximated T/N ratios of tumor models 0.9 cm and 1.2 cm but overestimated the other three tumor models. The results in Figure 4 demonstrated that if detection capability is emphasized, OSEM (BW 0.17 cycles/pixel) or OSEM (no BW), which produced greater T/N ratios than BW (0.10 cycles/pixel), should be preferred; on the other hand, if accurate quantification of T/N ratios is emphasized, then the reconstruction algorithm setting should be altered based on the size of the tumor-to-be-imaged. Therefore, how to determine appropriate prefiltering deserves further attention.

To achieve the full recovery of the prepared "tumors" in the phantom images, a "hot spot" of 5 cm in diameter (3-fold greater than the SPECT resolution), on which partial volume effect could be avoided theoretically, was inserted into the torso phantom. The results of T/Ns greater than the true value (5.0) in OSEM reconstruction demonstrated that OSEM might have overestimated the T/N ratios of big tumors in clinical practice. However, this overestimation might be useful to observe those tumors with  $^{201}\text{Tl}$  low uptake, especially during radiotherapy and/or chemotherapy.

One limitation of this study is the paradoxical results obtained between the clinical study and phantom study. Although no significantly greater T/N ratios by OSEM than FBP in the patient study were obtained, relatively higher T/N ratios were obtained in OSEM than in FBP in the phantom study, when BW of cut-off frequency of 0.10 cycles/pixel was incorporated. The result that T/N ratios of OSEM with BW (0.17 cycles/pixel) were slightly greater than those without BW is also unacceptable. The low radioactive counts per pixel in the background ROI in

the phantom study might be one of the reasons leading to such paradoxical results. Further study is required to prove or disprove this explanation.

In summary, OSEM reconstruction without prefilter incorporation could delineate clearly tumors larger than 2 cm in diameter but could not achieve significantly greater T/N ratios than FBP without prefiltering. BW might be necessary in OSEM reconstruction for small lesions; however the possible influence of prefilter setting on T/N calculation needs further study.

## ACKNOWLEDGMENT

The authors thank Dr. Jun Hashimoto for his helpful technical assistance and valuable discussions.

## REFERENCES

1. Stjernsward SK. Lung cancer. In: Hansen HH, ed. *Basic and clinical concepts of lung cancer*. Norwell, MA; Kluwer, 1989: 1-4.
2. Matsuno S, Tanabe M, Kawasaki Y, Satoh K, Urrutia AE, Ohkawa M, et al. Effectiveness of planar image and single photon emission tomography of thallium-201 compared with gallium-67 in patients with primary lung cancer. *Eur J Nucl Med* 1992; 19: 86-95.
3. Abdel-Dayem HM, Scott A, Macapinlac H, Larson S. Tracer imaging in lung cancer. *Eur J Nucl Med* 1994; 21: 57-81.
4. Chin BB, Zukerberg BW, Buchpiguel C, Alavi A. Thallium-201 uptake in lung cancer. *J Nucl Med* 1995; 36: 1514-1519.
5. Ochi H, Sawa H, Fukuda T, Inoue Y, Nakajima H, Masuda Y, et al. Thallium-201-chloride thyroid scintigraphy to evaluate benign and/or malignant nodules. *Cancer* 1982; 50: 236-240.
6. Suga K, Kume N, Orihashi N, Nishigauchi K, Uchisako H, Matsumoto T, et al. Difference in  $^{201}\text{Tl}$  accumulation on single photon emission computed tomography in benign and malignant lesions. *Nucl Med Commun* 1993; 14: 1071-1078.
7. Ando A, Ando I, Katayama M, Sanada S, Hiraki T, Mori H, et al. Biodistributions of  $^{201}\text{Tl}$  in tumor-bearing animals and inflammatory lesion induced animals. *Eur J Nucl Med* 1987; 12: 567-572.
8. Oriuchi N, Nomura M, Shibasaki T, Ohye C, Watanabe N, Tateno M, et al. Clinical evaluation of thallium-201 SPECT in supratentorial gliomas: relationship to histologic grade, prognosis and proliferative activity. *J Nucl Med* 1993; 34: 2085-2089.
9. Ishibashi M, Taguchi A, Sugita Y, Morita S, Kawamura S, Umezaki N, et al. Thallium-201 in brain tumors: relationship between tumor cell activity in astrocytic tumor and proliferating cell nuclear antigen. *J Nucl Med* 1995; 36: 2201-2206.
10. Tonami N, Shuke N, Yokoyama K, Seki H, Takayama T, Kinuya S, et al. Thallium-201 single photon emission computed tomography in the evaluation of suspected lung cancer. *J Nucl Med* 1989; 30: 997-1004.
11. Takekawa H, Takaoka K, Tsukamoto E, Kanegae K, Miller

- F, Kawakami Y. Thallium-201 single photon computed tomography as an indicator of prognosis for patients with lung carcinoma. *Cancer* 1997; 80: 198–203.
12. Shepp L, Logan B. The Fourier reconstruction of a head section. *IEEE Trans Nucl Sci* 1974; 21: 21–43.
  13. Lonnew M, Borbath I, Bol A, Coppens A, Sibomana M, Bausart R, et al. Attenuation correction in whole body FDG oncological studies: the role of statistical reconstruction. *Eur J Nucl Med* 1999; 40: 591–598.
  14. Bai J, Hashimoto J, Suzuki T, Nakahara T, Kubo A, Iwanaga S, et al. Comparison of image reconstruction algorithms in myocardial perfusion scintigraphy. *Ann Nucl Med* 2001; 15: 79–83.
  15. Case JA, Licho R, King MA, Weaver JP. Bone SPECT of the spine: a comparison of attenuation correction techniques. *J Nucl Med* 1999; 40: 604–613.
  16. Dey D, Slomka PJ, Hahn LJ, Cloiber R. Comparison of ordered subsets expectation maximization and Chang's attenuation correction method in quantitative cardiac SPECT: a phantom study. *Nucl Med Comm* 1998; 19: 1149–1157.
  17. Blocklet D, Seret A, Popa N, Schoutens A. Maximum-likelihood reconstruction with ordered subsets in bone SPECT. *J Nucl Med* 1999; 40: 1978–1984.
  18. Lalush DS, Tsui BMW. Performance of ordered-subset reconstruction algorithms under conditions of extreme attenuation and truncation in myocardial SPECT. *J Nucl Med* 2000; 41: 737–744.
  19. Visvikis D, Cheze-LeRest C, Costa DC, Bomanji J, Gacinovic S, Ell PJ. Influence of OSEM and segmented attenuation correction in the calculation of standardized uptake values for [ $^{18}\text{F}$ ]FDG PET. *Eur J Nucl Med* 2001; 28: 1326–1335.